Published in final edited form as:
Toxicol Appl Pharmacol. 2014 December 1; 281(2): 203–210. doi:10.1016/j.taap.2014.10.004.

Enhanced susceptibility of ovaries from obese mice to 7,12-dimethylbenz[a]anthracene-induced DNA damage

Shanthi Ganesan, **Jackson Nteeba**, and **Aileen F. Keating***
Department of Animal Science, Iowa State University, Ames, IA 50011, USA.

Abstract

7,12-dimethylbenz[a]anthracene (DMBA) depletes ovarian follicles and induces DNA damage in extra-ovarian tissues, thus, we investigated ovarian DMBA-induced DNA damage. Additionally, since obesity is associated with increased offspring birth defect incidence, we hypothesized that a DMBA-induced DNA damage response (DDR) is compromised in ovaries from obese females. Wild type (lean) non agouti (a/a) and KK.Cg-Ay/J heterozygote (obese) mice were dosed with sesame oil or DMBA (1mg/kg; intraperitoneal injection) at 18 wks of age, for 14 days. Total ovarian RNA and protein were isolated and abundance of Ataxia telangiectasia mutated (*Atm*), X-ray repair complementing defective repair in chinese hamster cells 6 (*Xrcc6*), Breast cancer type 1 (*Brca1*), Rad 51 homolog (*Rad51*), Poly [ADP-ribose] polymerase 1 (*Parp1*) and Protein kinase, DNA-activated, catalytic polypeptide (*Prkdc*) were quantified by RT-PCR or Western blot. Phosphorylated histone H2AX (γH2AX) level was determined by Western blotting. Obesity decreased ($P < 0.05$) basal protein abundance of PRKDC and BRCA1 proteins but increased ($P < 0.05$) γH2AX and PARP1 proteins. Ovarian ATM, XRCC6, PRKDC, RAD51 and PARP1 proteins were increased ($P < 0.05$) by DMBA exposure in lean mice. A blunted DMBA-induced increase ($P < 0.05$) in XRCC6, PRKDC, RAD51 and BRCA1 was observed in ovaries from obese mice, relative to lean counterparts. Taken together, DMBA exposure induced γH2AX as well as the ovarian DDR, supporting that DMBA causes ovarian DNA damage. Additionally, ovarian DDR was partially attenuated in obese females raising concern that obesity may be an additive factor during chemical-induced ovotoxicity.

Keywords

Ovary; DMBA; Ovotoxicity; DNA double strand breaks; DNA repair; Obesity

***Corresponding author:** Aileen F. Keating, Ph.D., Department of Animal Science, Iowa State University, Ames, IA 50011. akeating@iastate.edu; Telephone number 1-515-294-3849; Fax number: 1-515-294-4471..
shanthig@iastate.edu
nteeba@iastate.edu
akeating@iastate.edu

Introduction

7,12-dimethylbenz[a]anthracene (DMBA) is a polycyclic aromatic hydrocarbon which destroys all follicle types leading to ovarian failure in mice and rats (Mattison and Schulman, 1980) and is one component liberated through cigarette smoke and car exhaust fumes (Gelboin, 1980). It is recognized that female smokers experience ovarian senescence at an earlier age than their non-smoking counterparts (Jick and Porter, 1977), and low level DMBA exposure caused follicle depletion in neonatal culture rat ovaries, raising concern that ovotoxicity can be induced at levels which may be representative of passive DMBA exposure (Madden *et al.*, 2014).

DMBA requires the action of ovarian enzymes cytochromes p450 (Cyp) isoforms 1A1 and 1B1 (Shimada *et al.*, 2003) and microsomal epoxide hydrolase (mEH) (Rajapaksa *et al.*, 2007; Igawa*et al.*, 2009; Madden *et al.*, 2014) for biotransformation to the ovotoxic metabolite, DMBA 3,4-diol, 1,2-epoxide, which is both carcinogenic and has the potential to form DNA adducts (Miyata*et al.*, 1999). DMBA exposure also induces the DNA damage response (DDR) in cultured neonatal rat ovaries, indicating that DNA damage is a potential mechanism by which DMBA induces its ovotoxic effects (Ganesan *et al.*, 2013).

Double-strand breaks (DSBs) in DNA are cytotoxic lesions, generated by ionizing radiation and man-made chemicals (van Gent *et al.*, 2001). DSB's can be sensed by a PI3K family member Ataxia telangiectasia mutated (ATM) protein (Norbury and Hickson, 2001; Yang *et al.*, 2003; Giunta *et al.*, 2010). ATM phosphorylates histone H2AX (γH2AX) which leads, within seconds, to recruitment of DNA repair molecules to the site of DSBs (Sedelnikova *et al.*, 2002; Svetlova*et al.*, 2010), thus γH2AX has become a gold standard marker for localizing DSBs. DNA DSB's pose a serious threat to both cell viability and genome stability if left unrepaired or repaired incorrectly, and could potentially lead to permanent damage with resulting negative consequences for gamete health (Petrillo *et al.*, 2011; Summers *et al.*, 2011). Two major pathways can repair DNA DSB's: Non-Homologous End Joining (NHEJ) (Chiruvella *et al.*, 2012) and Homologous Recombination (HR) (Scully *et al.*, 1997). Key signaling molecules involved in NHEJ repair include the X-ray repair complementing defective repair in Chinese hamster cells 6 and 5 (XRCC6 and XRCC5) heterodimer which recognizes and binds to the DSB, recruiting protein kinase DNA-activated, catalytic polypeptide (PRKDC) to the DSB ends (Calsou *et al.*, 2003; Dobbs *et al.*, 2010; Chiruvella *et al.*, 2012). During HR, breast cancer type 1 (BRCA1) can be phosphorylated by ATM and co-localizes with RAD51 recombinase (RAD51) at the site of DNA damage to induce DSB repair (Scully *et al.*, 1997).

Approximately 65% of women in the United States are overweight or obese (Flegal *et al.*, 2010) and the associated reproductive complications include menstrual cycle disturbances, ovulatory dysfunction, infertility, decreased conception, early pregnancy loss and congenital abnormalities in offspring (Cardozo *et al.*, 2012; Sauber-Schatz *et al.*, 2012). Obesity has been associated with altered insulin and insulin growth factor (IGF) signaling (Qatanani and Lazar, 2007), likely due to obese females being typically hyperinsulinemic with concomitant insulin resistance (Kashyap, 2007; Choi and Kim, 2010). Insulin serves as a regulator of hepatic enzymes involved in the metabolism of xenobiotics (Woodcroft and Novak, 1999),

mediated, at least partly, through activation of phosphatidylinositol-3 kinase (PI3K) and variety of downstream effectors including protein kinase B (Akt) (Niswender *et al.*, 2003; Kim and Novak, 2007). Insulin increases mEH protein expression in primary cultured rat hepatocytes (Kim *et al.*, 2003). Also, increased ovarian PI3K signaling and mEH have been demonstrated in mice fed a high fat diet until obese (Nteeba*et al*., 2013). The obese lethal yellow mouse was also found to have both higher basal levels of mEH and greater mEH induction in response to DMBA exposure (Nteeba *et al.*, 2014). These data suggest that ovarian tissue from obese females could have potentially greater exposure to the ovotoxic metabolite of DMBA, due to higher levels of ovarian mEH, and thus greater DMBA bioactivation to a metabolite that interacts with DNA (Miyata *et al.*, 1999). The objective of this study was therefore to investigate ovarian DMBA-induced DNA damage as evidenced by γH2AX appearance and induction of the DDR in both lean and obese mice.

Methods and Materials

Reagents

7,12-dimethylbenz[a]anthracene (DMBA; CAS # 57-97-6), sesame oil (CAS # 8008-74-0), 2-β-mercaptoethanol, 30% acrylamide/0.8% bisacrylamide, ammonium persulphate, glycerol, N′N′N′N′-Tetramethylethylenediamine (TEMED), Tris base, Tris HCL, Sodium chloride, Tween-20 were purchased from Sigma-Aldrich Inc. (St Louis, MO). RNeasy Mini kit, QIA shredder kit, RNeasy Min Elute kit, and Quantitect TM SYBR Green PCR kit were purchased from Qiagen Inc (Valencia, CA). All primers were purchased from the Iowa State University DNA facility. All primary antibodies were purchased from Abcam (Cambridge, MA) with the exception of the BRCA1(C-20) primary antibody which was from Santa Cruz Biotechnology (Santa Cruz, CA). RNA *later* was obtained from Ambion Inc. (Austin, TX). Goat anti-mouse and anti-rabbit secondary antibodies were obtained from Santa Cruz Biotechnology (Santa Cruz, CA). Ponceau S was from Fisher Scientific. ECL plus chemical luminescence detection kit was obtained from GE Healthcare, Amersham (Buckinghamshire, UK).

Animals

Ovarian tissue was obtained as part of a larger study by our group (Nteeba *et al.*, 2014). Briefly, four week old female wild type normal non-agouti (a/a; designated lean; n = 10) and agouti lethal yellow (KK.Cg-Ay/J; designated obese; n = 10) were purchased from Jackson laboratories (Bar Harbor, ME 002468). All animals were housed in cages under a 12 h light/dark photoperiod with the temperature between 70-73°F and humidity approximately 20-30%. The animals were provided with a standard diet (Teklad 2014 global 14% protein rodent maintenance diet) with *ad libitum* access to food and water until 18 weeks of age. All animal experimental procedures were approved by the Iowa State University Animal Care and Use Committee.

In vivo DMBA exposure

Both lean and obese mice were intraperitoneally (i.p.) dosed with sesame oil (SO) or DMBA (95%; 1mg/kg per day) for 14 days. This dose was chosen based on a report that it caused follicular loss in the ovary (Mattison and Thorgeirsson, 1979). Mice were euthanized 3 days

after the end of dosing in their pro-estrus phase. One ovary from each mouse was fixed in 4% paraformaldehyde and one ovary was preserved at −80°C for RNA and protein isolation. This ovary was powdered and half used to isolate RNA and protein was isolated from the other half. As a note, one ovary from an obese DMBA-treated female could not be localized therefore the final number in this group was n = 4, with n = 5 for all other treatments. No difference in body weights due to DMBA exposure was observed although the lethal yellow mice had higher body weights (Nteeba *et al.*, 2014). DMBA reduced ovarian weight and volume in both lean and obese mice, relative to vehicle treated mice, and ovarian weight and volume were lower in obese DMBA-treated relative to lean DMBA-treated mice (Nteeba *et al.*, 2014).

RNA was isolated from all ovaries (n = 4-5) using an RNeasy Mini kit (Qiagen) and the concentration was determined using an ND-1000 Spectrophotometer (λ = 260/280nm; NanoDrop technologies, Inc., Wilmington, DE) (n = 3). Total RNA (200 ng) was reverse transcribed to cDNA utilizing the Superscript III One-Step RT-PCR (Qiagen). Three randomly chosen cDNA samples per treatment were diluted (1:20) in RNase-free water and amplified on an Eppendorf PCR Master cycler using Quantitect SYBR Green PCR kit (Qiagen). Primers for *Atm, Brca1, Prkdc, Parp1, Rad51, Xrcc6* and *Gapdh* were designed by Primer 3 Input Version (0.4.0) and are listed in Table 1. The regular cycling program consisted of a 15 min hold at 95°C and 45 cycles of denaturing at 95°C for 15 s, annealing at 58°C for 15 s, and extension at 72°C for 20 s at which point data were acquired. There was no difference in *Gapdh* mRNA expression between treatments, thus each sample was normalized to *Gapdh* before quantification. Quantification of fold-change in gene expression was performed using the $2^{-\Delta\Delta Ct}$ method (Livak and Schmittgen, 2001; Pfaffl, 2001).

Protein isolation and Western blotting

Protein was isolated from whole ovaries (n = 4-5) that had been homogenized in tissue lysis buffer containing protease and phosphatase inhibitors as previously described (Thompson *et al.*, 2005). Briefly, homogenized samples were placed on ice for 30 min, followed by two rounds of centrifugation at 10,000 rpm for 15 min. The protein concentration was measured using a standard BCA protocol. SDS-PAGE was used to separate three randomly chosen protein homogenates per treatment which were then transferred to a nitrocellulose membrane. Membranes were blocked for 1 h in 5 % milk in Tris-buffered saline containing tween 20, followed by incubation with one of: anti-rabbit PARP1 antibody (1:200), anti-rabbit phosphorylated H2AX antibody (γH2AX; 1:100), anti-mouse ATM antibody (1:100), anti-mouse RAD51 antibody (1:500), anti-mouse XRCC6 antibody (1:100), anti-rabbit BRCA1 antibody (1:500), or anti-rabbit PRKDC antibody (1:100) for 36 h at 4°C. Following three washes in TTBS (1X), membranes were incubated with species-specific secondary antibodies (1:2000) for 1 h at room temperature. Membranes were washed 3X in TTBS and incubated in chemiluminescence detection substrate (ECL plus) for 5 min followed by X-ray film exposure. Densitometry of the appropriate bands was performed using ImageJ software (NCBI). Chemical exposures can impact traditional housekeeping protein abundance (our unpublished data), thus equal protein loading was confirmed by Ponceau S staining of total protein and protein level was normalized to Ponceau S densitometry values

Statistical analysis

Sufficient animal numbers were included for statistical analysis of the data. Raw data were analyzed by unpaired t-test (comparison of two samples) or one-way ANOVA (comparison of multiple samples) analysis with the Tukey pairwise comparison using Graphpad Prism 5.04 software. Values are expressed as mean ± SE; n = 3. A *P*-value < 0.05 was considered a significant difference between treatments, while $P < 0.1$ was considered a trend towards a difference.

Results

Effect of DMBA on ovarian γH2AX in lean and obese mice

γH2AX protein was absent in lean control-treated ovaries but was evident ($P < 0.05$) in obese ovaries that had received sesame oil. γH2AX protein level was increased ($P < 0.05$) by DMBA exposure in both lean and obese mice compared to their respective control-treated ovaries (Figure 1A). Relative to lean mice when compared to its respective control, the DMBA-induced increase in γH2AX protein was lower in ovaries from obese mice (Figure 1B).

Impact of DMBA exposure on ovarian *Atm* abundance in lean and obese mice

Basal *Atm* mRNA levels were lower ($P < 0.05$) in ovaries from obese relative to lean mice. In lean mice, ovarian *Atm* mRNA levels were decreased ($P < 0.05$) by DMBA exposure compared to control-treated animals. In contrast, in obese mice, DMBA exposure increased ($P < 0.05$) ovarian *Atm* mRNA levels relative to control-treated obese mice (Figure 2A). There was no difference in basal ovarian ATM protein levels between lean and obese mice. Nor in the ATM protein response to DMBA which was elevated in both the lean and obese females (Figure 2B, C).

DMBA-induction of ovarian *Xrcc6* mRNA and protein in lean and obese mice

Basal levels of *Xrcc6* mRNA were lower ($P < 0.05$) in obese compared to lean mouse ovaries. In lean mice, levels of *Xrcc6* mRNA were increased by DMBA exposure while, in contrast, DMBA exposure did not impact *Xrcc6* in obese ovaries (Figure 3A). There was no impact of obesity on ovarian XRCC6 protein. In both lean and obese mice, relative to control-treated animals, levels of ovarian XRCC6 protein were increased ($P < 0.05$) by DMBA exposure. Interestingly, relative to lean DMBA-treated ovaries, DMBA-induced XRCC6 protein expression was lower ($P < 0.05$) in obese ovaries (Figure 3B, C).

Response of ovarian *Prkdc* mRNA and protein to DMBA exposure in lean and obese mice

Basal levels of *Prkdc* mRNA were lower ($P < 0.05$) in obese compared to lean ovaries. In lean mice, levels of *Prkdc* mRNA were decreased ($P < 0.05$) by DMBA exposure compared to control-treated ovaries. In contrast, DMBA exposure increased ($P < 0.05$) *Prkdc* mRNA level in ovaries from obese mice, compared to obese control-treated animals (Figure 4A). Basal PRKDC protein levels were lower ($P < 0.05$) in obese relative to lean ovaries. In lean mice, relative to control-treated animals, ovarian PRKDC protein was increased ($P < 0.05$)

by DMBA exposure (Figure 4B, C), but this response was absent in the obese female ovaries.

Impact of DMBA exposure on ovarian *Brca1* mRNA and protein in lean and obese mice

Lower ($P < 0.05$) levels of basal *Brca1* mRNA were observed in obese ovaries relative to lean ovaries. In both lean and obese mice, levels of *Brca1* mRNA were increased ($P < 0.05$) by DMBA exposure compared to their respective control treatment, however, obesity resulted in a blunted DMBA-induced *Brca1* mRNA increase (Figure 5A). Basal BRCA1 protein levels were lower ($P < 0.05$) in obese relative to lean ovaries. In obese mice, relative to control-treated animals, levels of ovarian BRCA1 protein were increased ($P < 0.05$) by DMBA exposure while no BRCA1 induction was observed in lean mice (Figure 5B, C).

Ovarian DMBA-induced *Rad51* mRNA and protein in lean and obese mice

No difference in basal *Rad51* mRNA abundance between lean and obese ovarian tissue was observed (Figure 6A). In lean mice, levels of *Rad51* mRNA was increased by DMBA exposure compared to control treatments, but this response was absent in obese ovaries (Figure 6A). There was no difference in basal RAD51 protein levels between lean and obese ovaries. In both lean and obese mice, RAD51 protein levels were increased ($P < 0.05$) by DMBA exposure compared to control treatments. Interestingly, the increase in RAD51 protein level after DMBA exposure was lower ($P < 0.05$) in the obese relative to lean ovaries (Figure 6B, C).

DMBA-induction of ovarian *Parp1* mRNA and protein in lean and obese mice

Higher basal levels of *Parp1* mRNA were noted in obese compared to lean ovaries. In lean and obese mice, levels of *Parp1* mRNA were increased ($P < 0.05$) by DMBA exposure compared to control treatments (Figure 7A). Basal PARP1 protein levels were higher in obese relative to lean ovaries. DMBA increased ($P < 0.05$) PARP1 protein in both lean and obese mice (Figure 7B, C).

Discussion

Obesity is a detrimental physiological state for oocyte quality and fertility (Wittemer *et al.*, 2000; Brewer and Balen, 2010). Maternal obesity also increases the risk of offspring birth defects (Watkins *et al.*, 2003). Additionally, obesity alters the ovarian response to chemical insult, as evidenced by the results observed with DMBA, a known ovarian toxicant (Nteeba *et al.*, 2014). DMBA depleted healthy follicles of all types in both lean and obese treated females compared to sesame-treated females (Nteeba *et al.*, 2014). No difference in DMBA-induced follicle depletion was observed between the lean and obese females likely due to the extensive DMBA damage that occurred in both, however ovarian weight was lower in the obese DMBA relative to the lean DMBA treated mice (Nteeba *et al*., 2014). These results indicate greater levels of DMBA-induced ovotoxicity in obese relative to lean mice, potentially through induction of DNA damage.

One mechanism to justify the potential for increased ovarian DNA damage caused by DMBA in obese mice is increased bioactivation of DMBA by the increased concentration of

ovarian mEH observed in obese mice (Nteeba *et al*., 2014). This increased mEH would generate more of the reactive diepoxide metabolite responsible for ovarian DNA damage (Miyata *et al*., 1999). Thus, ovarian DNA damage was assessed in ovaries of control and DMBA treated mice by monitoring molecular events involved in the DDR in response to formation of DSBs.

The action of ATM, which is recruited upon DSB formation to phosphorylate downstream cellular effector molecules results in either cell cycle arrest to accomodate DNA repair (Canman*et al.*, 1998; Lee and Paull, 2007) or apoptosis (Stankovic *et al.*, 2002) (Waster and Ollinger, 2009). DMBA exposure decreased *Atm* mRNA level in lean ovaries while the opposite was the case in obese ovaries. Despite this, increased ATM protein was observed in both lean and obese ovaries upon DMBA exposure indicating that ovarian DNA damage is imparted by DMBA exposure. Activation of ATM, associated with apoptotic oocyte death, has been previously observed during doxorubicin exposure in embryonic stem cells (Soleimani *et al.*, 2011). While it is difficult to conclude whether our conflicting effects of DMBA exposure in lean and obese ovaries on *Atm* mRNA levels indicate different mechanisms of regulation during obesity, it is clear that DMBA exposure increased ovarian ATM protein regardless of metabolic status, supporting that DMBA induces ovarian DNA damage in an *in vivo* model, consistant with our previous data in cultured neonatal rat ovaries (Ganesan *et al*., 2013).

When a DSB occurs, ATM phosphorylates H2AX (γH2AX), a sensitive marker of DSBs (Bouquet *et al.*, 2006; Mah *et al.*, 2010). We demonstrate increased γH2AX protein due to DMBA exposure regardless of the presence of obesity. These data are also in agreement with our previous study that found activated γH2AX protein in neonatal rat ovaries that had been exposure to DMBA (Ganesan *et al.*, 2013). Interestingly, low levels of γH2AX protein were observed during obesity, independent of DMBA exposure, which may indicate that low level DNA damage is present in ovarian tissue of obese females. DNA damage in peripheral lymphocytes of obese and overweight italian children has been demonstrated (Jungheim *et al.*, 2010), thus our data are in agreement with these studies. Taken together, these data further support that DMBA exposure induces ovarian DNA damage, and that the ovary is responsive to such an insult.

γH2AX recruits XRCC6 and PRKDC to repair DNA by the NHEJ pathway (Summers *et al.*, 2011). *Xrcc6* mRNA was increased by DMBA exposure in lean ovaries but no change was observed with obesity, though a lower basal level was present. In contrast to mRNA data, XRCC6 protein was increased by DMBA in both lean and obese ovaries but this increase appeared to be blunted due to obesity. This lowered response could be due to basal DNA damage that is seemingly present in ovarian tissue during obesity as suggested by the observed γH2AX. Defective DNA repair and chromosomal instability due to decreased XRCC6 have been reported in embryonic cells (Gu *et al.*, 1997). In addition, suppressed XRCC6 leads to DNA damage and reactive oxygen species-induced endoplasmic reticulum stress in Toll like receptor (TLR) 4 mutant liver cells, ultimately leading to induction of the ATM-PRKDC protein complex as well as induction of PARP1, resulting in apoptosis of precancerous hepatocytes (Wang *et al.*, 2013). *Prkdc* mRNA expression was decreased by DMBA exposure in lean but increased in obese ovaries. In contrast, despite their being

reduced basal levels of PRKDC protein in obese relative to lean mice, PRKDC protein induction by DMBA exposure was observed in both lean and obese mice. Inhibition of PRKDC reduces γH2AX and the HR repair mechanism in a medaka embryonic cell line (Urushihara *et al.*, 2012). Thus, our data suggest that increased PRKDC by DMBA exposure might play a pro-apoptotic role in ovarian tissue.

PARP1 is involved in DNA damage-induced cell apoptosis (D'Amours *et al.*, 1999) and DMBA has been shown to increase PARP1 expression prior to follicle loss in neonatal rat ovaries (Ganesan *et al.*, 2013). DMBA increased both *Parp1* mRNA and protein in lean and obese ovaries, with ovaries from obese mice having higher basal levels of *Parp1*. Elevated *Parp1* could play a role in DMBA-induced ovotoxicity, since PARP1 inhibition previously protected against cisplastin-induced renal damage and inflammation (Kim *et al.*, 2012). Interestingly, the mitochondrial apoptotic pathway mediated by caspase 9 is constitutively activated in oocytes and contibutes to the elimination of oocytes with meiotic errors through the cleavage and activation of PARP1 (Ene *et al.*, 2013). Thus, increased PARP1 observed in our study could mediate increased DMBA-induced ovotoxicity.

DMBA has been shown to induce ROS generation and DNA damage in *Brca1* knock down MCF10A cells (Kang *et al.*, 2013). In agreement with our previpous study demonstrating increased *Brca1* in neonatal rat ovaries exposure to DMBA (Ganesan *et al.*, 2013), we found increased DMBA-induced *Brca1* mRNA in ovaries of lean mice but this response was partly attentuated in ovaries from obese mice. In contrast, BRCA1 protein was increased in ovaries from obese but not lean ovaries due to DMBA exposure. Interestingly, and in contrast to the observed increased γH2AX, we noted that basal *Brca1* mRNA and protein abundance was lower due to obesity. Reduced *Brca1* is associated with an increased risk of hereditary breast and ovarian cancer (Robson *et al.*, 1998; Kauff *et al.*, 2002). BRCA1 controls the mitotic checkpoint complex, and loss of this control can lead to mitotic errors contributing to neoplasia in ovarian cystadenoma cells (Yu *et al.*, 2012). Further, women with *Brca1* mutations can experience earlier ovarian senescence and develop ovarian cancer at younger ages (Rzepka-Górska *et al.*, 2006). Impairment of BRCA1-related DNA DSB repair has been associated with accelerated loss of the ovarian follicular reserve and with accumulation of DSB in human oocytes, suggesting that DNA DSB repair efficiency is an important determinant of oocyte aging in women (Titus *et al.*, 2013). Interestingly, RAD51 interacts with BRCA1 during DDR and DMBA exposure increased RAD51 protein abundance in both prostate tissue (Xu *et al.*, 2002) and in cultured neonatal rat ovaries (Ganesan *et al.*, 2013). In this study, DMBA exposure increased *Rad51* mRNA levels in lean but not obese mice. Furthermore, ovarian RAD51 protein was upregulated by DMBA in the lean females but a reduced response was observed in ovaries from obese females. These impacts of obesity on the DMBA-induced BRCA1 and RAD51 proteins could contribute to negative impacts on female reproduction.

In summary, our results support that DMBA exposure induces DSB formation in the ovary and the DDR is activated in ovarian tissue of exposed mice. We provide novel data that the ovaries from obese female mice were observed to have a low level of γH2AX protein therein, indicating that DNA damage, outside of ovotoxicant exposure, may be present. Also, levels of some ovarian DDR proteins (XRCC6, BRCA1, PRKDC and RAD51) were

blunted due to obesity, suggesting perhaps a reduced ability to respond to chemical-induced DNA damage. Interestingly, we found a disconnect between mRNA and protein levels in some genes (*Atm* and *Prkdc*), perhaps indicating that a delay in transcript processing occurs in ovaries from obese mice, or that other regulators of gene expression are affected, potentially including microRNA as was previously found in a high fat feeding-induced obesity mouse model (Nteeba *et al.*, 2013). These findings underscoring the importance of investigating translational as well as transcriptional effects of obesity. We found that immunolocalization of the proteins examined correlated well with the Western blotting data (supplemental Figure 1) and future studies are required to address both post-translational modifications in the proteins described herein and to quantifiy the changes in ovarian cells in which these modifications occur. It is important to note that this study represents a single snapshot in time of the DMBA-induced ovarian DDR. Taken together, a higher sensitivity to and suceptibility for DMBA-induced ovotoxicity effects in obese females is supported. As smokers have an increased exposure to DMBA, it will be important to determine if obese smokers show evidence of impaired ovarian function that is greater than that of non-obese smokers.

Supplementary Material

Refer to Web version on PubMed Central for supplementary material.

Acknowlegements

The project described was supported by award number R00ES016818 to AFK. The content is solely the responsibility of the authors and does not necessarily represent the official views of the National Institute of Environmental Health Sciences or the National Institutes of Health.

Abbreviations

DMBA	7,12-dimethylbenz[a]anthracene
DDR	DNA damage response
DSBs	Double-strand breaks
NHEJ	Non-Homologous End Joining
HR	Homologous Recombination
TLR	Toll like receptor
Cyp	Cytochromes p450
IGF	Insulin growth factor
PI3K	Phosphatidylinositol-3 kinase
Akt	Protein kinase B
ATM	Ataxia telangiectasia mutated
XRCC6	X-ray repair complementing defective repair in chinese hamster cells 6
BRCA1	Breast cancer type 1

RAD 51	Rad 51 homolog
PARP1	Poly [ADP-ribose] polymerase 1
PRKDC	Protein kinase
DNA-activated	catalytic polypeptide
γH2AX	Phosphorylated histone H2AX
mEH	microsomal Epoxide Hydrolase
TEMED	N′N′N′N′-Tetramethylethylenediamine

References cited

Bouquet F, Muller C, Salles B. The Loss of γH2AX Signal is a Marker of DNA Double Strand Breaks Repair Only at Low Levels of DNA Damage. Cell Cycle. 2006; 5:1116–1122. [PubMed: 16721046]

Brewer CJ, Balen AH. The adverse effects of obesity on conception and implantation. Reproduction. 2010; 140:347–364. [PubMed: 20395425]

Calsou P, Delteil C, Frit P, Drouet J, Salles B. Coordinated assembly of Ku and p460 subunits of the DNA-dependent protein kinase on DNA ends is necessary for XRCC4-ligase IV recruitment. J. Mol. Biol. 2003; 326:93–103. [PubMed: 12547193]

Canman CE, Lim D-S, Cimprich KA, Taya Y, Tamai K, Sakaguchi K, Appella E, Kastan MB, Siliciano JD. Activation of the ATM Kinase by Ionizing Radiation and Phosphorylation of p53. Science. 1998; 281:1677–1679. [PubMed: 9733515]

Cardozo ER, Neff LM, Brocks ME, Ekpo GE, Dune TJ, Barnes RB, Marsh EE. Infertility patients' knowledge of the effects of obesity on reproductive health outcomes. Am. J. Obstet. Gynecol. 2012; 207:509, e501–509, e510. [PubMed: 22981319]

Chiruvella KK, Sebastian R, Sharma S, Karande AA, Choudhary B, Raghavan SC. Time-dependent predominance of nonhomologous DNA end-joining pathways during embryonic development in mice. J. Mol. Biol. 2012; 417:197–211. [PubMed: 22306462]

Choi K, Kim YB. Molecular mechanism of insulin resistance in obesity and type 2 diabetes. Korean J. Int. Med. 2010; 25:119–129.

D'Amours D, Desnoyers S, D'Silva I, Poirier GG. Poly(ADP-ribosyl)ation reactions in the regulation of nuclear functions. Biochem. J. 1999; 342:249–268. [PubMed: 10455009]

Dobbs TA, Tainer JA, Lees-Miller SP. A structural model for regulation of NHEJ by DNA-PKcs autophosphorylation. DNA Repair (Amst). 2010; 9:1307–1314. [PubMed: 21030321]

Ene AC, Park S, Edelmann W, Taketo T. Caspase 9 is constitutively activated in mouse oocytes and plays a key role in oocyte elimination during meiotic prophase progression. Develop. Biol. 2013; 377:213–223. [PubMed: 23384561]

Flegal KM, Carroll MD, Kit BK, Ogden CL. Prevalence and trends in obesity among US adults, 1999-2008. JAMA. 2010; 303:235–241. [PubMed: 20071471]

Ganesan S, Bhattacharya P, Keating AF. 7,12-Dimethylbenz[a]anthracene exposure induces the DNA repair response in neonatal rat ovaries. Toxicol. Appl. Pharmacol. 2013; 272:690–696. [PubMed: 23969067]

Gelboin HV. Benzo[alpha]pyrene metabolism, activation and carcinogenesis: role and regulation of mixed-function oxidases and related enzymes. Physiol. Rev. 1980; 60:1107–1166. [PubMed: 7001511]

Giunta S, Belotserkovskaya R, Jackson SP. DNA damage signaling in response to double-strand breaks during mitosis. J. Cell Biol. 2010; 190:197–207. [PubMed: 20660628]

Gu Y, Jin S, Gao Y, Weaver DT, Alt FW. Ku70-deficient embryonic stem cells have increased ionizing radiosensitivity, defective DNA end-binding activity, and inability to support V(D)J recombination. PNAS. 1997; 94:8076–8081. [PubMed: 9223317]

Igawa Y, Keating AF, Rajapaksa KS, Sipes IG, Hoyer PB. Evaluation of ovotoxicity induced by 7, 12-dimethylbenz[a]anthracene and its 3,4-diol metabolite utilizing a rat in vitro ovarian culture system. Toxicol. Appl. Pharmacol. 2009; 234:361–369. [PubMed: 19027032]

Jick H, Porter J. Relation between smoking and age of natural menopause. Report from the Boston Collaborative Drug Surveillance Program, Boston University Medical Center. Lancet. 1977; 1:1354–1355. [PubMed: 69066]

Jungheim ES, Schoeller EL, Marquard KL, Louden ED, Schaffer JE, Moley KH. Diet-Induced Obesity Model: Abnormal Oocytes and Persistent Growth Abnormalities in the Offspring. Endocrinology. 2010; 151:4039–4046. [PubMed: 20573727]

Kang HJ, Hong YB, Yi YW, Cho CH, Wang A, Bae I. The correlations between BRCA1 defect and environmental factors in the risk of breast cancer. Tox. Sci. 2013; 38:355–361.

Kashyap SR, Defronzo RA. The insulin resistance syndrome: physiological considerations. Diab. Vasc. Dis. Res. 2007; 4:13–19. [PubMed: 17469039]

Kauff ND, Satagopan JM, Robson ME, Scheuer L, Hensley M, Hudis CA, Ellis NA, Boyd J, Borgen PI, Barakat RR, Norton L, Castiel M, Nafa K, Offit K. Risk-Reducing Salpingo-oophorectomy in Women with a BRCA1 or BRCA2 Mutation. New Engl. J. Med. 2002; 346:1609–1615. [PubMed: 12023992]

Kim J, Long KE, Tang K, Padanilam BJ. Poly(ADP-ribose) polymerase 1 activation is required for cisplatin nephrotoxicity. Kidney Int. 2012; 82:193–203. [PubMed: 22437413]

Kim SK, Novak RF. The role of intracellular signaling in insulin-mediated regulation of drug metabolizing enzyme gene and protein expression. Pharmacol. Ther. 2007; 113:88–120. [PubMed: 17097148]

Kim SK, Woodcroft KJ, Kim SG, Novak RF. Insulin and glucagon signaling in regulation of microsomal epoxide hydrolase expression in primary cultured rat hepatocytes. Drug Metab. Dispos. 2003; 31:1260–1268. [PubMed: 12975336]

Lee JH, Paull TT. Activation and regulation of ATM kinase activity in response to DNA double-strand breaks. Oncogene. 2007; 26:7741–7748. [PubMed: 18066086]

Livak KJ, Schmittgen TD. Analysis of Relative Gene Expression Data Using Real-Time Quantitative PCR and the 2−ΔΔCT Method. Methods. 2001; 25:402–408. [PubMed: 11846609]

Madden JA, Hoyer PB, Devine PJ, Keating AF. Acute 7,12-dimethylbenz[a]anthracene exposure causes differential concentration-dependent follicle depletion and gene expression in neonatal rat ovaries. Toxicol. Appl. Pharmacol. 2014; 276(3):179–187. [PubMed: 24576726]

Mah LJ, El-Osta A, Karagiannis TC. [gamma]H2AX: a sensitive molecular marker of DNA damage and repair. Leukemia. 2010; 24:679–686. [PubMed: 20130602]

Mattison DR, Thorgeirsson SS. Ovarian Aryl Hydrocarbon Hydroxylase Activity and Primordial Oocyte Toxicity of Polycyclic Aromatic Hydrocarbons in Mice. Cancer Res. 1979; 39:3471–3475. [PubMed: 113091]

Mattison DR, Schulman JD. How xenobiotic chemicals can destroy oocytes. Contemp. Obstet. Gynecol. 1980; 15:157.

Miyata M, Kudo G, Lee Y-H, Yang TJ, Gelboin HV, Fernandez-Salguero P, Kimura S, Gonzalez FJ. Targeted Disruption of the Microsomal Epoxide Hydrolase Gene. J. Biol. Chem. 1999; 274:23963–23968. [PubMed: 10446164]

Niswender KD, Morrison CD, Clegg DJ, Olson R, Baskin DG, Myers MG, Seeley RJ, Schwartz MW. Insulin Activation of Phosphatidylinositol 3-Kinase in the Hypothalamic Arcuate Nucleus: A Key Mediator of Insulin-Induced Anorexia. Diabetes. 2003; 52:227–231. [PubMed: 12540590]

Norbury CJ, Hickson ID. Cellular Responses to DNA Damage. Ann. Rev. Pharmacol. Toxicol. 2001; 41:367–401. [PubMed: 11264462]

Nteeba J, Ganesan S, Keating AF. Impact of Obesity on Ovotoxicity Induced by 7,12-Dimethylbenz[a]anthracene in Mice. Biol Reprod. 2014

Nteeba J, Ross JW, Perfield JW II, Keating AF. High fat diet induced obesity alters ovarian phosphatidylinositol-3 kinase signaling gene expression. Reprod. Toxicol. 2013; 42:68–77. [PubMed: 23954404]

Petrillo SK, Desmeules P, Truong T-Q, Devine PJ. Detection of DNA damage in oocytes of small ovarian follicles following phosphoramide mustard exposures of cultured rodent ovaries in vitro. Toxicol. Appl. Pharmacol. 2011; 253:94–102. [PubMed: 21439308]

Pfaffl MW. A new mathematical model for relative quantification in real-time RT-PCR. Nucleic Acids Res. 2001; 29:e45. [PubMed: 11328886]

Qatanani M, Lazar MA. Mechanisms of obesity-associated insulin resistance: many choices on the menu. Genes Dev. 2007; 21:1443–1455. [PubMed: 17575046]

Rajapaksa KS, Sipes IG, Hoyer PB. Involvement of microsomal epoxide hydrolase enzyme in ovotoxicity caused by 7,12-dimethylbenz[a]anthracene. Tox. Sci. 2007; 96:327–334.

Robson M, Gilewski T, Haas B, Levin D, Borgen P, Rajan P, Hirschaut Y, Pressman P, Rosen PP, Lesser ML, Norton L, Offit K. BRCA-associated breast cancer in young women. J. Clin. Oncol. 1998; 16:1642–1649. [PubMed: 9586873]

Rzepka-Górska I, Tarnowski B, Chudecka-Głaz A, Górski B, Zielińska D, Tołoczko-Grabarek A. Premature Menopause in Patients with BRCA1 Gene Mutation. Breast Cancer Res. Treat. 2006; 100:59–63. [PubMed: 16773440]

Sauber-Schatz EK, Sappenfield W, Grigorescu V, Kulkarni A, Zhang Y, Salihu HM, Rubin LP, Kirby RS, Jamieson DJ, Macaluso M. Obesity, Assisted Reproductive Technology, and Early Preterm Birth—Florida, 2004–2006. Am. J. Epidemiol. 2012; 176:886–896. [PubMed: 23097258]

Scully R, Chen J, Plug A, Xiao Y, Weaver D, Feunteun J, Ashley T, Livingston DM. Association of BRCA1 with Rad51 in mitotic and meiotic cells. Cell. 1997; 88:265–275. [PubMed: 9008167]

Sedelnikova OA, Rogakou EP, Panyutin IG, Bonner WM. Quantitative detection of (125) IdU-induced DNA double-strand breaks with gamma-H2AX antibody. Radiation Res. 2002; 158:486–492. [PubMed: 12236816]

Shimada T, Sugie A, Shindo M, Nakajima T, Azuma E, Hashimoto M, Inoue K. Tissue-specific induction of cytochromes P450 1A1 and 1B1 by polycyclic aromatic hydrocarbons and polychlorinated biphenyls in engineered C57BL/6J mice of arylhydrocarbon receptor gene. Toxicol. Appl. Pharmacol. 2003; 187:1–10. [PubMed: 12628579]

Soleimani R, Heytens E, Darzynkiewicz Z, Oktay K. Mechanisms of chemotherapy-induced human ovarian aging: double strand DNA breaks and microvascular compromise. Aging (Albany NY). 2011; 3:782–793. [PubMed: 21869459]

Stankovic T, Stewart GS, Fegan C, Biggs P, Last J, Byrd PJ, Keenan RD, Moss PAH, Taylor AMR. Ataxia telangiectasia mutated–deficient B-cell chronic lymphocytic leukemia occurs in pregerminal center cells and results in defective damage response and unrepaired chromosome damage. Blood. 2002; 99:300–309. [PubMed: 11756185]

Summers KC, Shen F, Sierra Potchanant EA, Phipps EA, Hickey RJ, Malkas LH. Phosphorylation: The Molecular Switch of Double-Strand Break Repair. Int. J. Proteo. 2011. 2011

Svetlova MP, Solovjeva LV, Tomilin NV. Mechanism of elimination of phosphorylated histone H2AX from chromatin after repair of DNA double-strand breaks. Mut. Res. 2010; 685:54–60. [PubMed: 19682466]

Thompson KE, Bourguet SM, Christian PJ, Benedict JC, Sipes IG, Flaws JA, Hoyer PB. Differences between rats and mice in the involvement of the aryl hydrocarbon receptor in 4-vinylcyclohexene diepoxide-induced ovarian follicle loss. Toxicol. Appl. Pharmacol. 2005; 203:114–123. [PubMed: 15710172]

Titus S, Li F, Stobezki R, Akula K, Unsal E, Jeong K, Dickler M, Robson M, Moy F, Goswami S, Oktay K. Impairment of BRCA1-Related DNA Double-Strand Break Repair Leads to Ovarian Aging in Mice and Humans. Science Trans. Med. 2013; 5:172ra121.

Urushihara Y, Kobayashi J, Matsumoto Y, Komatsu K, Oda S, Mitani H. DNA-PK inhibition causes a low level of H2AX phosphorylation and homologous recombination repair in Medaka (Oryzias latipes) cells. Biochem. Biophys. Res. Comm. 2012; 429:131–136. [PubMed: 23142596]

van Gent DC, Hoeijmakers JH, Kanaar R. Chromosomal stability and the DNA double-stranded break connection. Nature reviews. Genetics. 2001; 2:196–206.

Wang Z, Lin H, Hua F, Hu Z.-w. Repairing DNA damage by XRCC6/KU70 reverses TLR4-deficiency-worsened HCC development via restoring senescence and autophagic flux. Autophagy. 2013; 9:925–927. [PubMed: 23518600]

Waster PK, Ollinger KM. Redox-Dependent Translocation of p53 to Mitochondria or Nucleus in Human Melanocytes after UVA-and UVB-Induced Apoptosis. J. Invest. Dermatol. 2009; 129:1769–1781. [PubMed: 19158844]

Watkins ML, Rasmussen SA, Honein MA, Botto LD, Moore CA. Maternal Obesity and Risk for Birth Defects. Pediatrics. 2003; 111:1152–1158. [PubMed: 12728129]

Wittemer C, Ohl J, Bailly M, Bettahar-Lebugle K, Nisand I. Does Body Mass Index of Infertile Women Have an Impact on IVF Procedure and Outcome? J. Asst. Reprod. Gene. 2000; 17:547–552.

Woodcroft KJ, Novak RF. Insulin Differentially Affects Xenobiotic-Enhanced, Cytochrome P-450 (CYP)2E1, CYP2B, CYP3A, and CYP4A Expression in Primary Cultured Rat Hepatocytes. J. Pharmacol. Exp. Therapeutics. 1999; 289:1121–1127.

Xu J, Osuga Y, Yano T, Morita Y, Tang X, Fujiwara T, Takai Y, Matsumi H, Koga K, Taketani Y, Tsutsumi O. Bisphenol A Induces Apoptosis and G2-to-M Arrest of Ovarian Granulosa Cells. Biochem. Biophys. Res. Commun. 2002; 292:456–462. [PubMed: 11906184]

Yang J, Yu Y, Hamrick HE, Duerksen-Hughes PJ. ATM, ATR and DNA-PK: initiators of the cellular genotoxic stress responses. Carcinogenesis. 2003; 24:1571–1580. [PubMed: 12919958]

Yu VM, Marion CM, Austria TM, Yeh J, Schönthal AH, Dubeau L. Role of BRCA1 in controlling mitotic arrest in ovarian cystadenoma cells. Int. J. Canc. 2012; 130:2495–2504.

Highlights

- DMBA induces markers of ovarian DNA damage
- Obesity induces low level ovarian DNA damage
- DMBA-induced DNA repair response is altered by obesity

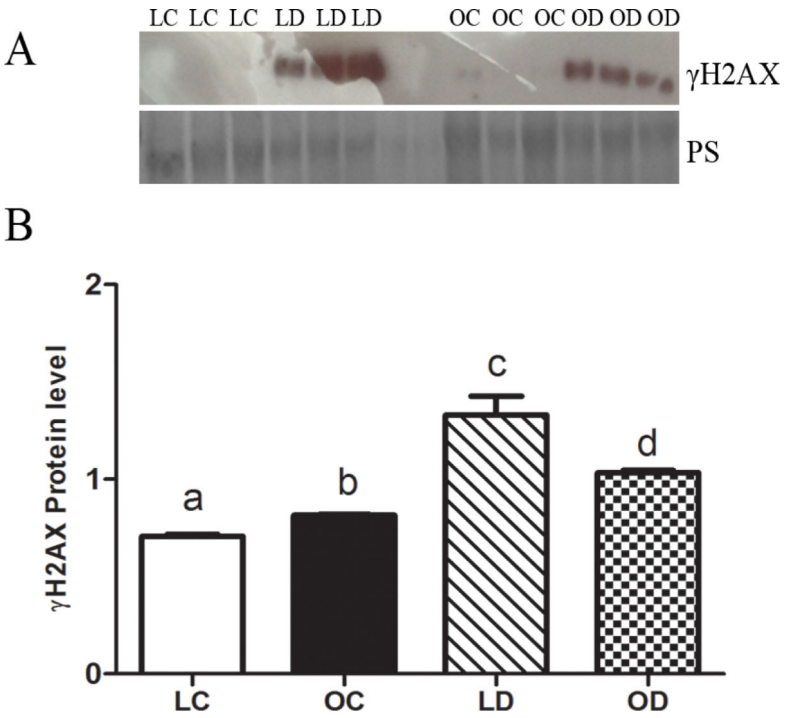

Figure 1. Effect of DMBA on ovarian H2AX phosphorylation in lean and obese mice

Lean and obese mice were dosed with sesame oil (CT) or DMBA (1 mg/kg; ip) for 14 days, followed by (A) Western blotting to detect γH2AX. Protein abundance was quantified using ImageJ software. Values are expressed as raw data mean ± SE; n=3. Different letters indicate $P < 0.05$.

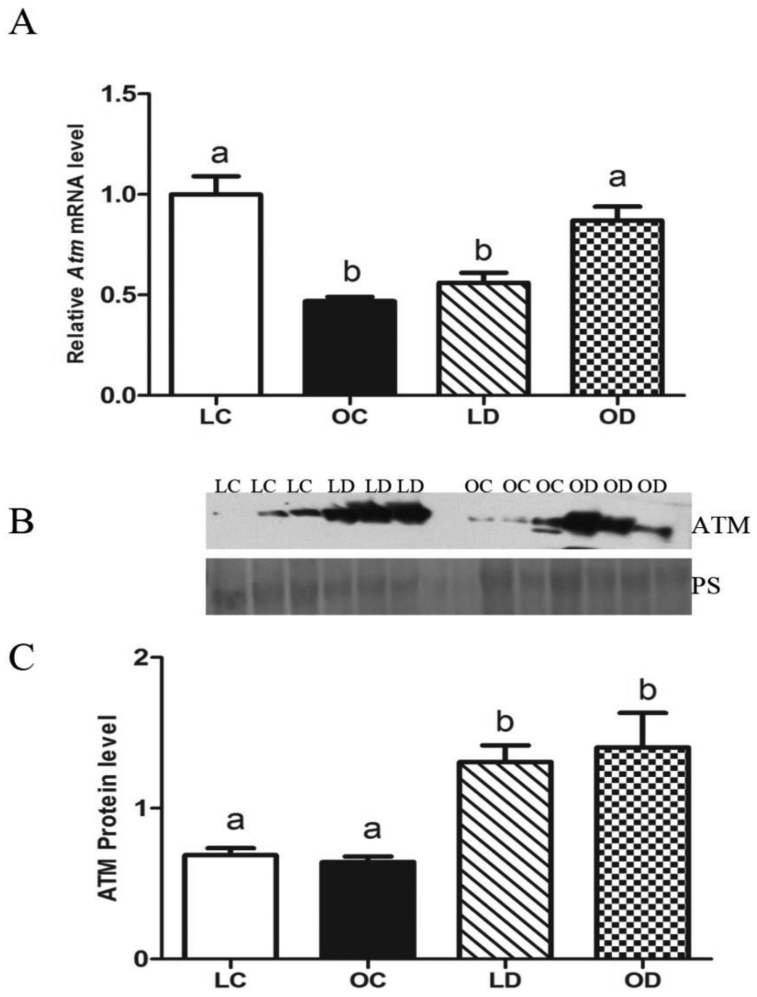

Figure 2. Impact of DMBA exposure on ovarian *Atm* abundance in lean and obese mice

Lean and obese mice were dosed with sesame oil (CT) or DMBA (1 mg/kg; ip) for 14 days, followed by RNA or protein isolation. qRT-PCR or Western blotting were performed to quantify *Atm* (A) mRNA or (B, C) protein abundance. (A) *Atm* was normalized to *Gapdh* for quantification, and values are reported as fold-change (n = 3) relative to lean CT ovaries (set at 1). (B) Protein abundance was quantified using ImageJ software; Lean control = LC; Lean DMBA = LD; Obese Control = OC, Obese DMBA = OD. Values are expressed as raw data mean ± SE; n=3. Different letters indicate $P < 0.05$.

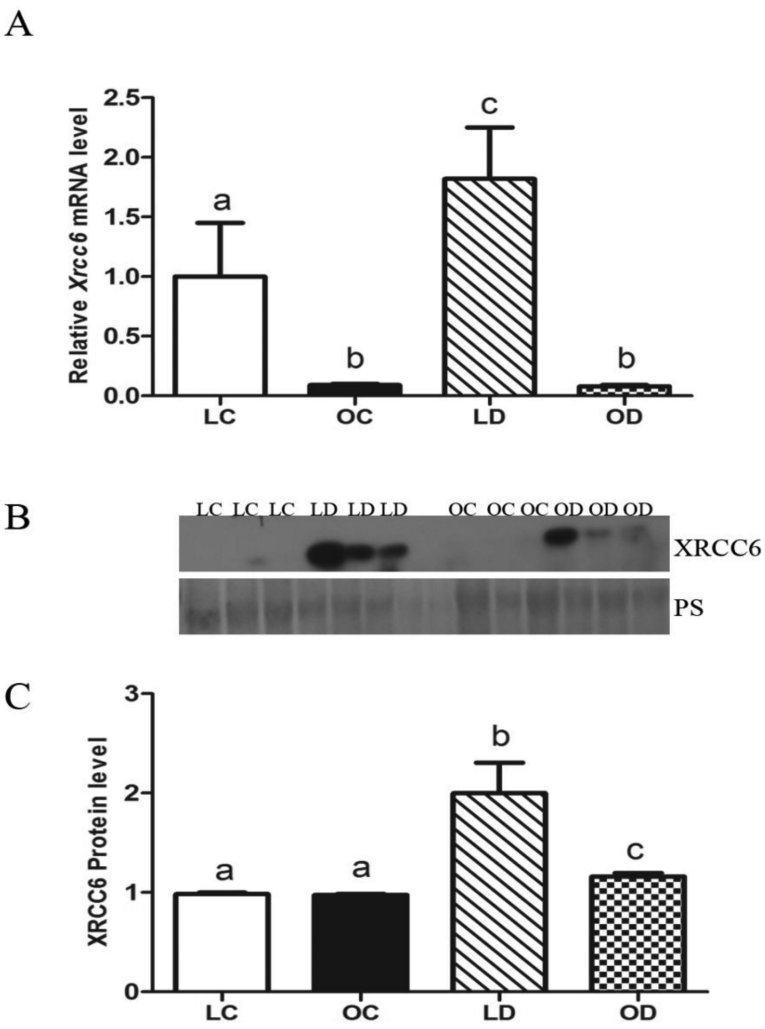

Figure 3. DMBA-induction of ovarian *Xrcc6* mRNA and protein in lean and obese mice

Lean and obese mice were dosed with sesame oil (CT) or DMBA (1 mg/kg; ip) for 14 days, followed by RNA or protein isolation. qRT-PCR or Western blotting were performed to quantify *Xrcc6* (A) mRNA or (B, C) protein abundance. (A) *Xrcc6* was normalized to *Gapdh* for quantification, and values are reported as fold-change (n = 3) relative to lean CT ovaries (set at 1). (B) Protein abundance was quantified using ImageJ software; Lean control = LC; Lean DMBA = LD; Obese Control = OC, Obese DMBA = OD. Values are expressed as raw data mean ± SE; n=3. Different letters indicate $P < 0.05$.

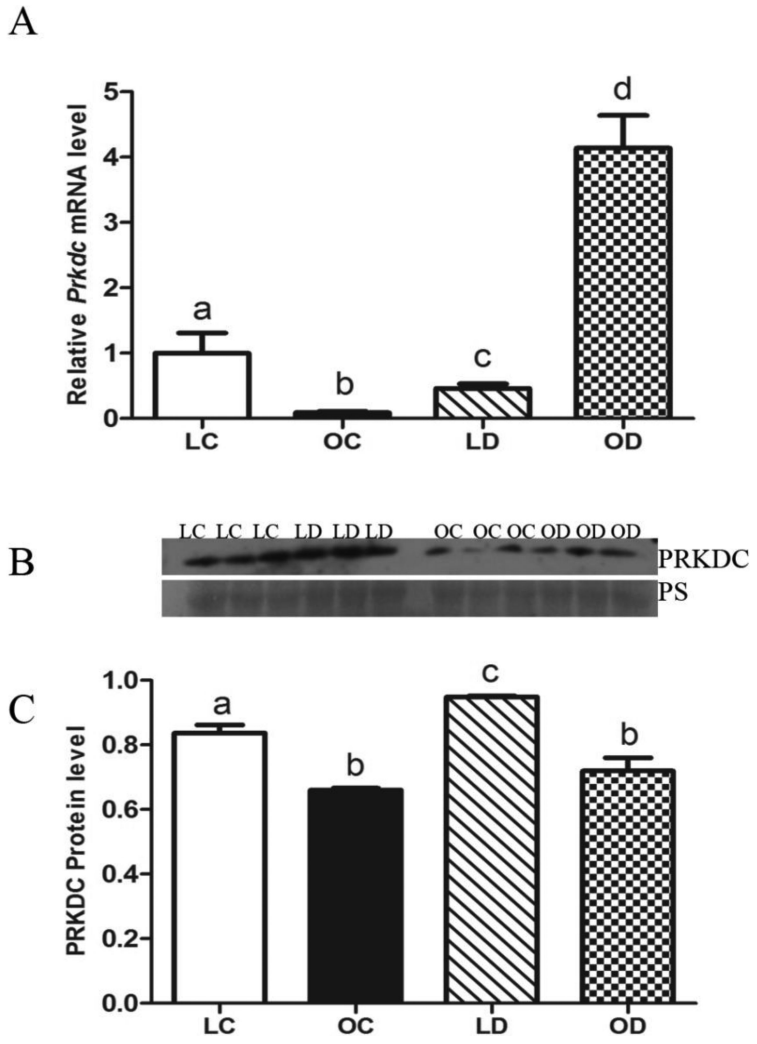

Figure 4. Response of ovarian *Prkdc* mRNA and protein to DMBA exposure in lean and obese mice

Lean and obese mice were dosed with sesame oil (CT) or DMBA (1 mg/kg; ip) for 14 days, followed by RNA or protein isolation. qRT-PCR or Western blotting were performed to quantify *Prkdc* (A) mRNA or (B, C) protein abundance. (A) *Prkdc* was normalized to *Gapdh* for quantification, and values are reported as fold-change (n = 3) relative to lean CT ovaries (set at 1). (B) Protein abundance was quantified using ImageJ software; Lean control = LC; Lean DMBA = LD; Obese Control = OC, Obese DMBA = OD. Values are expressed as raw data mean ± SE; n=3. Different letters indicate $P < 0.05$.

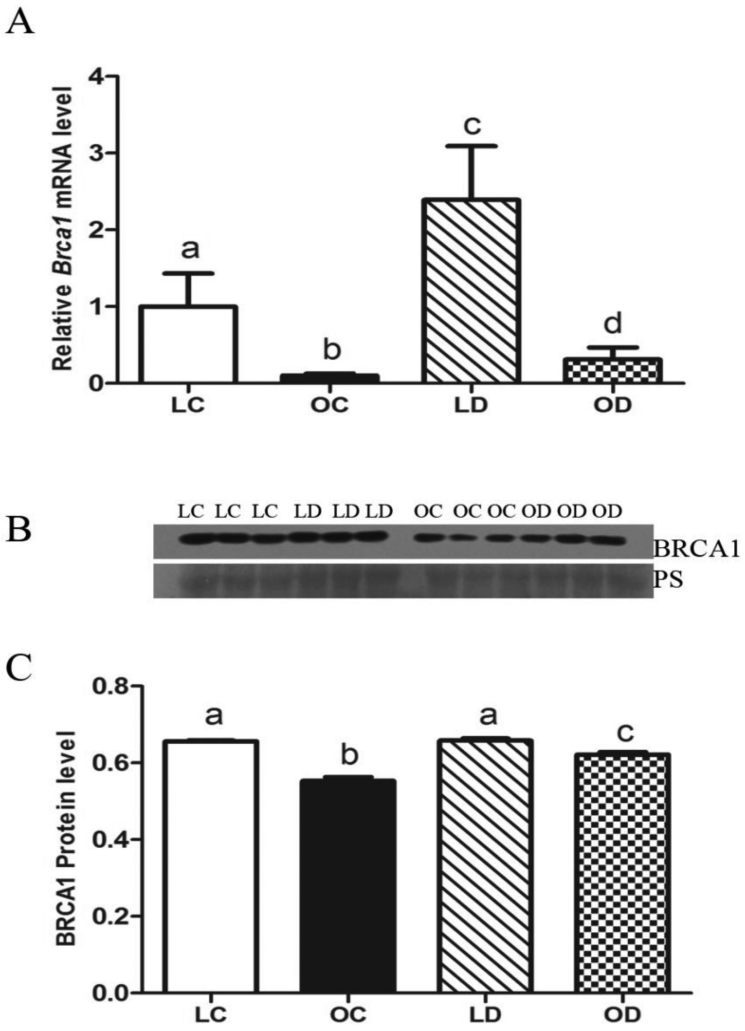

Figure 5. Impact of DMBA exposure on ovarian *Brca1* mRNA and protein in lean and obese mice

Lean and obese mice were dosed with sesame oil (CT) or DMBA (1 mg/kg; ip) for 14 days, followed by RNA or protein isolation. qRT-PCR or Western blotting were performed to quantify *Brca1* (A) mRNA or (B, C) protein abundance. (A) *Brca1* was normalized to *Gapdh* for quantification, and values are reported as fold-change (n = 3) relative to lean CT ovaries (set at 1). (B) Protein abundance was quantified using ImageJ software; Lean control = LC; Lean DMBA = LD; Obese Control = OC, Obese DMBA = OD. Values are expressed as raw data mean ± SE; n=3. Different letters indicate $P < 0.05$.

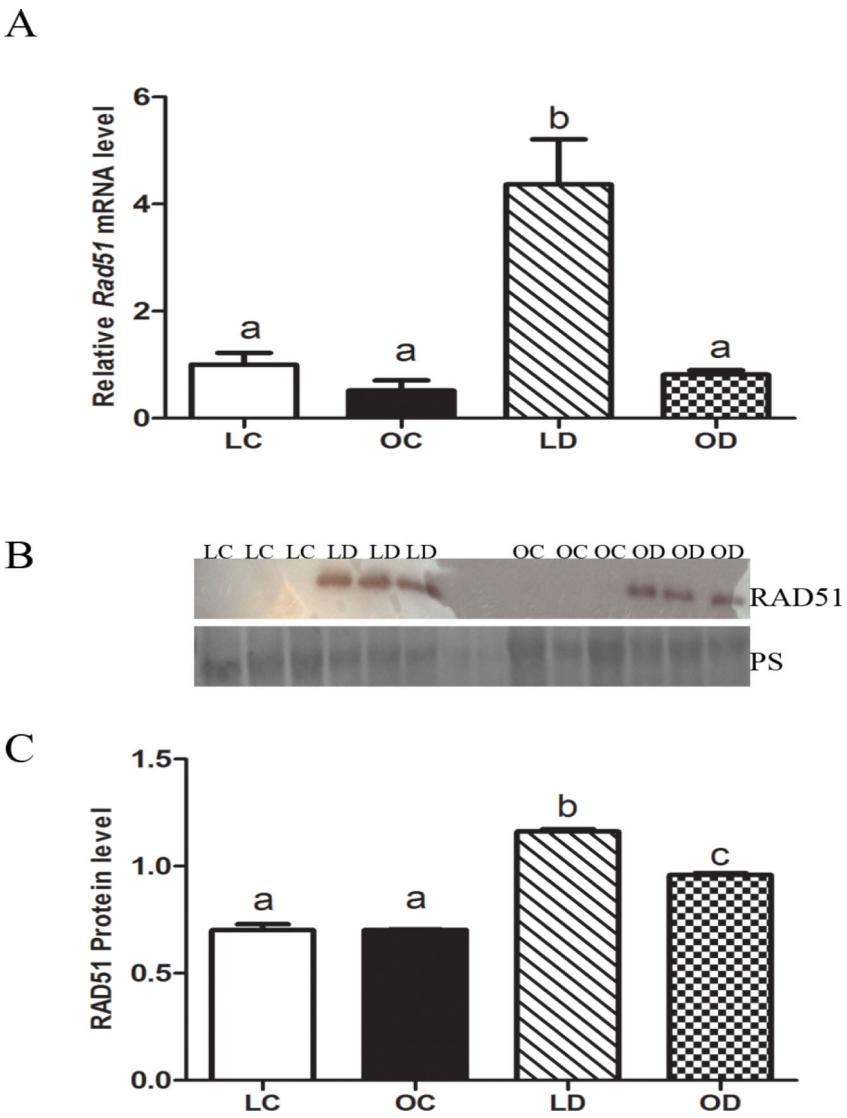

Figure 6. Ovarian DMBA-induced *Rad51* mRNA and protein in lean and obese mice

Lean and obese mice were dosed with sesame oil (CT) or DMBA (1 mg/kg; ip) for 14 days, followed by RNA or protein isolation. qRT-PCR or Western blotting were performed to quantify *Rad51* (A) mRNA or (B, C) protein abundance. (A) *Rad51* was normalized to *Gapdh* for quantification, and values are reported as fold-change (n = 3) relative to lean CT ovaries (set at 1). (B) Protein abundance was quantified using ImageJ software; Lean control = LC; Lean DMBA = LD; Obese Control = OC, Obese DMBA = OD. Values are expressed as raw data mean ± SE; n=3. Different letters indicate $P < 0.05$.

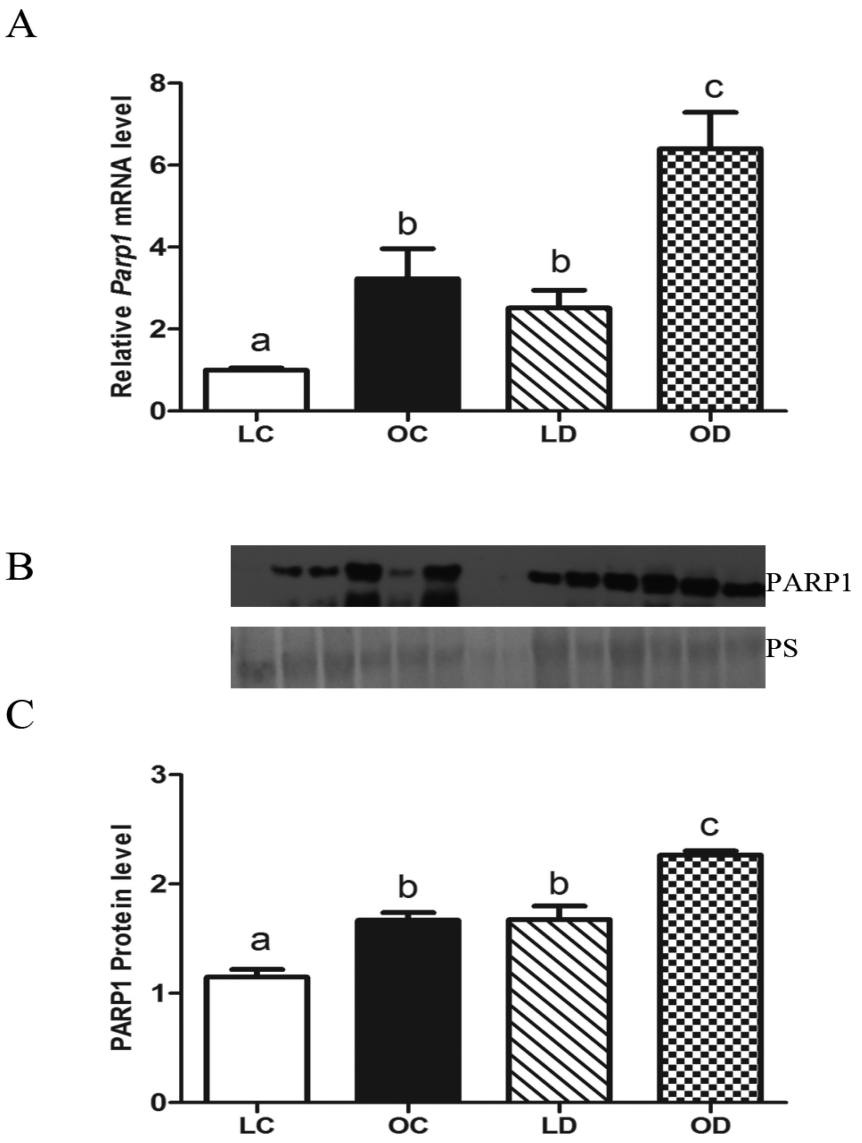

Figure 7. DMBA-induction of ovarian *Parp1* mRNA and protein in lean and obese mice

Lean and obese mice were dosed with sesame oil (CT) or DMBA (1 mg/kg; ip) for 14 days, followed by RNA or protein isolation. qRT-PCR or Western blotting were performed to quantify *Parp1* (A) mRNA or (B, C) protein abundance. (A) *Parp1* was normalized to *Gapdh* for quantification, and values are reported as fold-change (n = 3) relative to lean CT ovaries (set at 1). (B) Protein abundance was quantified using ImageJ software; Lean control = LC; Lean DMBA = LD; Obese Control = OC, Obese DMBA = OD. Values are expressed as raw data mean ± SE; n=3. Different letters indicate $P < 0.05$.

Table 1

Gene	Forward primer	Reverse primer
Atm	TCAGCAGCACCTCTGATTCTT	AGACAGACATGCTGCCTCCT
Brcal	CCCTCTTAGTCTGCTGAGCT	CCTTTGGGTGGCTGTACTGA
Parpl	AAGTGCCAGTGTCAAGGAGA	ACAGGGAGCAAAAGGGAAGA
Prkdc	GCCACAGACCCCAATATCCT	TATCTGACCATCTCGCCAGC
Rad51	ATCCCTGCATGCTTGTTCTC	CTGCAGCTGACCATAACGAA
Xrcc6	GATCTGACACTGCCCAAGGT	TGCTTCTTCGGTCCACTCTT